

Reactivity of B(C₆F₅)₃ with Simple Early Transition Metal Alkoxides: Alkoxide-Aryl Exchange, THF Ring-Opening, or Acetonitrile CC Coupling

Christian Lorber,* Robert Choukroun, and Laure Vendier

Laboratoire de Chimie de Coordination, CNRS UPR 8241 (Lié par Convention à l'Université Paul Sabatier et à l'Institut National Polytechnique), 205 Route de Narbonne, 31077 Toulouse Cedex 04, France

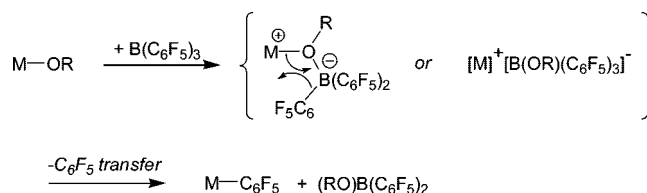
Received March 12, 2008

Treatment of the titanium(IV) and vanadium(IV) alkoxide complexes M(OPr^{*t*})₄ [M = Ti, V] with B(C₆F₅)₃ results in alkoxide-aryl exchange and formation of the organometallic dimer complexes [M(OPr^{*t*})₂(μ-OPr^{*t*})(C₆F₅)₂] (M = Ti (**1**), V (**2**)). In comparison, the reaction between B(C₆F₅)₃ and Zr(OBu^{*t*})₄ in pentane, followed by recrystallization in acetonitrile-THF solutions, affords the unexpected trimeric zirconium salt [Zr₃(OBu^{*t*})₆(μ₂-OBu^{*t*})₃(μ₃-OBu^{*t*})(μ₃-OCH₂CH₂CH₂CH₃)] [B(C₆F₅)₄] (**3**), which proceeds through a redox reaction involving the borane and the THF solvent. In the presence of CH₃CN, a tetranuclear complex formulated as [Zr₂(OBu^{*t*})₅(μ-OBu^{*t*})₂(μ-N,N'-N(H)C(CH₃)=C(H)C≡N)]₂ (**5**) is obtained, which results from a C,C coupling reaction between two acetonitrile molecules. When Zr(OBu^{*t*})₄ is treated with (HO)B(C₆F₅)₂, a dimer complex formulated as [Zr(OBu^{*t*})₂(μ-O-OB(OBu^{*t*})(C₆F₅)₂-κ²-O,O)]₂ (**7**) is formed that contains an unusual ligand bonding mode. The molecular structures of **1**, **2**, **3**, **5**, and **7** as well as the adduct B(C₆F₅)₃·THF (**4**) and [Zr(OBu^{*t*})₃(μ-OBu^{*t*})₂(μ-N≡CCH₃)] (**6**) have been determined by X-ray diffraction.

Introduction

The chemistry of the strongly Lewis acidic tris(pentafluorophenyl)borane B(C₆F₅)₃ is the subject of numerous applications. Although the main interest was its established role in the formation of cationic derivatives for polymerization, different organic, organometallic, and catalytic applications have been reported in the past few years.^{1–4} In our group, we have used B(C₆F₅)₃ in conjunction with early transition metal group 4 and 5 precursors to afford new and original organometallic complexes related to alkyl abstraction,⁵ reactivity of small molecules (CO,^{6,7} water^{8,9}) and nitriles.^{10–15} During this research, while attempting to generate metal-oxo·B(C₆F₅)₃ adducts or cationic species from oxo-vanadium(V) amido or alkoxo precursors treated with B(C₆F₅)₃, we found with others that in certain alkoxide complexes an exchange reaction between a C₆F₅ group of B(C₆F₅)₃ and an alkoxy ligand attached to a metal can occur, which results in the formation of an organometallic complex containing a metal-C₆F₅ moiety, as depicted in Scheme 1.^{16–19} Particularly, the reaction of [VO(OCH₂CF₃)₃]₂ in pentane with

Scheme 1. Alkoxide-Aryl Exchange Reaction



2 equiv of B(C₆F₅)₃ afforded the organometallic vanadium dimer complex [VO(μ-OCH₂CF₃)(OCH₂CF₃)₂(C₆F₅)₂]₂,¹⁶ a rare example of a structurally established alkyl-vanadium(V) complex.²⁰ The alkoxide-aryl exchange reaction presumably proceeds through a zwitterionic [M-μ-OR-B(C₆F₅)₃] adduct or a cationic [M]⁺[B(OR)(C₆F₅)₃]⁻ intermediate (Scheme 1). Our preliminary results prompted us to further investigate the reactivity of other homoleptic early transition metal alkoxides with B(C₆F₅)₃; in particular, we were interested in attempting to isolate the elusive intermediate in this reaction (zwitterionic

* Corresponding author. E-mail: lorber@lcc-toulouse.fr. Phone: (+33) 5 61 33 31 44. Fax: (+33) 5 61 55 30 03.

(1) Erker, G. *Dalton Trans.* **2005**, 1883–1890.
 (2) Focante, F.; Mercandelli, P.; Sironi, A.; Resconi, L. *Coord. Chem. Rev.* **2006**, *250*, 170–188.
 (3) Piers, W. E. *Adv. Organomet. Chem.* **2005**, *52*, 1–76.
 (4) Piers, W. E.; Chivers, T. *Chem. Soc. Rev.* **1997**, *23*, 345–354.
 (5) Choukroun, R.; Lorber, C.; Donnadiou, B. *Organometallics* **2002**, *21*, 1124–1126.
 (6) Choukroun, R.; Lorber, C.; Lepetit, C.; Donnadiou, B. *Organometallics* **2003**, *22*, 1995–1997.
 (7) Choukroun, R.; Lorber, C.; Donnadiou, B. *Organometallics* **2004**, *23*, 1434–1437.
 (8) Choukroun, R.; Lorber, C.; Vendier, L. *Eur. J. Inorg. Chem.* **2004**, 317–321.
 (9) Choukroun, R.; Lorber, C.; Vendier, L.; Lepetit, C. *Organometallics* **2006**, *25*, 1551–1553.
 (10) Choukroun, R.; Lorber, C.; Donnadiou, B. *Chem.—Eur. J.* **2002**, *8*, 2700–2704.

(11) Choukroun, R.; Lorber, C.; Vendier, L.; Donnadiou, B. *Organometallics* **2004**, *23*, 5488–5492.

(12) Choukroun, R.; Lorber, C.; Vendier, L. *Organometallics* **2007**, *26*, 3784–3790.

(13) Choukroun, R.; Lorber, C. *Eur. J. Inorg. Chem.* **2005**, 4683–4692.

(14) Choukroun, R.; Lorber, C.; Vendier, L. *Organometallics* **2007**, *26*, 3604–3606.

(15) Choukroun, R.; Lorber, C.; de Caro, D.; Vendier, L. *Organometallics* **2006**, *25*, 4243–4246.

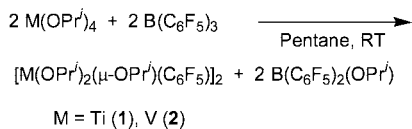
(16) Wolff, F.; Choukroun, R.; Lorber, C.; Donnadiou, B. *Eur. J. Inorg. Chem.* **2003**, 628–632.

(17) Hair, G. S.; Cowley, A. H.; Gordon, J. D.; Jones, J. N.; Jones, R. A.; Macdonald, C. L. B. *Chem. Commun.* **2003**, 424–425.

(18) Klosin, J.; Roof, G. R.; Chen, E. Y. X.; Abboud, K. A. *Organometallics* **2000**, *19*, 4684–4686.

(19) Walker, D. A.; Woodman, T. J.; Hughes, D. L.; Bochmann, M. *Organometallics* **2001**, *20*, 3772–3776.

(20) Lorber, C. Vanadium. In *Comprehensive Organometallic Chemistry III*; Crabtree R. H., Mingos, D. M. P., Eds.; Elsevier: Oxford: 2007; Vol. 5, pp 1–60.

Scheme 2. Synthesis of Complexes 1 and 2

or cationic species). Herein we report the reactivity of simple early transition metal alkoxide complexes $\text{M}(\text{OR})_4$ (M = Ti, Zr, V) with $\text{B}(\text{C}_6\text{F}_5)_3$. As part of this study, we also describe the reaction of $\text{Zr}(\text{O}i\text{Bu})_4$ with $(\text{HO})\text{B}(\text{C}_6\text{F}_5)_2$ and the molecular structure of the adduct $\text{B}(\text{C}_6\text{F}_5)_3 \cdot (\text{THF})$ and the complex $[\text{Zr}(\text{O}i\text{Bu})_3(\mu\text{-O}i\text{Bu})(\mu\text{-N}\equiv\text{CCH}_3)]_2$.

Alkoxide Exchange Reactions between $\text{M}(\text{OPr}^i)_4$ (M = Ti, V) and $\text{B}(\text{C}_6\text{F}_5)_3$. Treatment of the tetra-alkoxides $\text{M}(\text{OPr}^i)_4$ (M = Ti, V) with 1 equiv of $\text{B}(\text{C}_6\text{F}_5)_3$, at room temperature in pentane, gives the related organometallic dimer complexes $[\text{Ti}(\text{OPr}^i)_2(\mu\text{-OPr}^i)(\text{C}_6\text{F}_5)_2]_2$ (**1**) and $[\text{V}(\text{OPr}^i)_2(\mu\text{-OPr}^i)(\text{C}_6\text{F}_5)_2]_2$ (**2**), as shown in Scheme 2. The reaction is accompanied by the formation of $\text{B}(\text{OPr}^i)(\text{C}_6\text{F}_5)_2$, which is easily removed by filtration of the reaction mixtures (due to its higher solubility in pentane), and identified by its characteristic signals in ^1H , ^{19}F , and ^{11}B NMR spectroscopic studies. Complex **1** was previously prepared from $\text{TiCl}(\text{OPr}^i)_3$ and LiC_6F_5 ,²¹ whereas the mixture of $\text{Ti}(\text{OPr}^i)_4/\text{B}(\text{C}_6\text{F}_5)_3$ was recently studied as effective catalyst for ring-opening polymerization of propylene oxide (from which $\text{B}(\text{OPr}^i)(\text{C}_6\text{F}_5)_2$ appeared to be the active species).²² Complex **2** is a paramagnetic $d^1\text{-}d^1$ complex presenting in its solution EPR spectrum (RT, toluene) the characteristic eight-band pattern for a V(IV) species ($g = 1.979$, $a(^{51}\text{V}) = 54.1$ G) and a magnetic moment μ_{eff} of $2.44 \mu_{\text{B}}$ (per dimer). These studies are in agreement with a $d^1\text{-}d^1$ species with two noninteracting electrons.

Under the above experimental conditions, the formation of complex **1** is too rapid to allow an intermediate to be detected. However, the analogous vanadium system proceeds differently. Indeed, a light blue pentane solution of $\text{V}(\text{OPr}^i)_4$ turned gray-brown instantly upon addition of $\text{B}(\text{C}_6\text{F}_5)_3$ to afford after a few minutes a dark red solution. Later, brown crystals of complex **2** were formed upon standing for 2 weeks at room temperature. Following the reaction by EPR spectroscopy in a sealed capillary tube (both in pentane and in toluene solutions) showed the very rapid decrease of the signal of paramagnetic $\text{V}(\text{OPr}^i)_4$ ($g = 1.971$, $a(^{51}\text{V}) = 70.7$ G) after addition of $\text{B}(\text{C}_6\text{F}_5)_3$ (95% of the signal of $\text{V}(\text{OPr}^i)_4$ has disappeared 4 min after the addition), which implies the formation of an EPR-silent intermediate species, which further evolved slowly (2 weeks), giving a new signal for EPR-active complex **2** ($g = 1.979$, and $a(^{51}\text{V}) = 54.1$ G). The formation of a diamagnetic intermediate was also corroborated by following the same reaction by multinuclear NMR spectroscopic methods (^1H , ^{19}F , ^{11}B , ^{51}V NMR in C_6D_6 solutions). After complete consumption of paramagnetic $\text{V}(\text{OPr}^i)_4$ (ca. after 10 min) it was possible to record spectra with sharp signals corresponding to $\text{B}(\text{OPr}^i)(\text{C}_6\text{F}_5)_2$ and a new complex, **I**. The ^{51}V NMR spectrum clearly demonstrates the formation of only one vanadium compound [$\delta = -742$ ppm ($w_{1/2} = 15$ Hz) for **I**, as compared to -630 ppm ($w_{1/2} = 180$ Hz) for $\text{V}(\text{OPr}^i)_4$]. This vanadium compound presents in its ^1H NMR spectrum signals characteristic of terminal and bridging isopropoxides in a ratio of 3:1, while ^{19}F and ^{11}B NMR spectra suggest the additional presence of a tetracoordinated boron

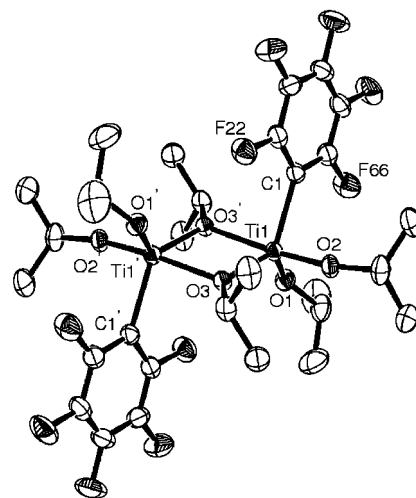


Figure 1. Molecular structure of **1**, showing 50% probability ellipsoids and partial atom-labeling scheme. Hydrogen atoms are omitted for clarity. Ti(1)–C(1) 2.1763(17), Ti(1)–O(1) 1.7651(13), Ti(1)–O(2) 1.7583(12), Ti(1)–O(3) 1.9420 (11), Ti1–O3' 2.0873(11), Ti(1)···Ti(1') 3.2299(6), O3–Ti1–O3' 73.53(5), Ti1–O3–Ti1' 106.47(5), O(2)–Ti(1)–O(1) 101.98(6), O(2)–Ti(1)–O(3) 99.93(5), O(1)–Ti(1)–O(3) 118.89(5), O(2)–Ti(1)–O(3') 167.35(6), O(1)–Ti(1)–O(3') 90.68(5), O(3)–Ti(1)–O(3') 73.49(5), O(2)–Ti(1)–C(1) 91.27(6), O(1)–Ti(1)–C(1) 108.61(7), O(3)–Ti(1)–C(1) 127.13(6).

species (^{19}F NMR: $\delta -131.2, -157.8, -164.4$; ^{11}B NMR: $\delta -5$). Unfortunately we were unable to obtain the intermediate **I** in a pure form due to its high solubility in pentane. While we expect this intermediate to be the zwitterionic $[\text{V}(\text{O}^i\text{Pr})_3(\mu\text{-O}^i\text{Pr}-\text{B}(\text{C}_6\text{F}_5)_3)]$ or cationic $[\text{V}(\text{O}^i\text{Pr})_3][\text{B}(\text{O}^i\text{Pr})(\text{C}_6\text{F}_5)_3]$,²³ we can probably rule out the second, as a cationic compound would probably be insoluble in pentane. Moreover, both above suggested zwitterionic or cationic possible intermediates would certainly be paramagnetic; therefore we propose **I** to be a dimer with bridging isopropoxides (as evidenced by ^1H NMR studies).²⁴

Crystals of **1** (colorless) and **2** (red-brown), suitable for X-ray diffraction analysis, were obtained from cold pentane solutions that allowed the determination of their molecular structure. The molecular structures of complexes **1** and **2** are presented in Figures 1 and 2, respectively, with selected bond distances and angles. During the course of our studies, Johnson and Davidson have reported the structure of **1** that crystallized in the same monoclinic space group ($P2_1/n$).²⁵ Therefore, we will discuss only the structure of the vanadium complex **2**, but details on the structure of **1** are given in the Supporting Information (the data are of better quality than those previously reported).

The molecular structure establishes that, in the solid state, **2** is a centrosymmetric dimeric complex composed of two $\text{V}(\text{OPr}^i)_2(\text{C}_6\text{F}_5)_2$ units linked by two bridging $-\text{OPr}^i$ ligands. In this respect, the overall structure of **2** resembles that of **1**. The coordination geometry of the vanadium centers is between a

(23) Chen et al. (see ref 22) showed that the aluminum analogue $\text{Al}(\text{C}_6\text{F}_5)_3$ forms the stable isopropoxy-bridged bimetallic adduct $[\text{Ti}(\text{O}^i\text{Pr})_3(\mu\text{-O}^i\text{Pr})(\text{Al}(\text{C}_6\text{F}_5)_3)]$, which is a monomer in the solid state.

(24) Selected examples of diamagnetic vanadium(IV) dimers: (a) Preuss, F.; Becker, H.; Kaub, J.; Sheldrick, W. S. *Z. Naturforsch.* **1988**, *43b*, 1195–1200. (b) Carrano, C. J.; Nunn, C. M.; Quan, R.; Bonadies, J. A.; Pecoraro, V. L. *Inorg. Chem.* **1990**, *29*, 944–951. (c) Lorber, C.; Choukroun, R.; Donnadieu, B. *Inorg. Chem.* **2002**, *41*, 4217–4226.

(25) Johnson, A. L.; Davidson, M. G.; Mahon, M. F. *Dalton Trans.* **2007**, 5405–5411.

(21) Rausch, M. D.; Gordon, H. B. *J. Organomet. Chem.* **1974**, *74*, 85–90.

(22) Rodriguez-Delgado, A.; Chen, E. Y. X. *Inorg. Chim. Acta* **2004**, *357*, 3911–3919.

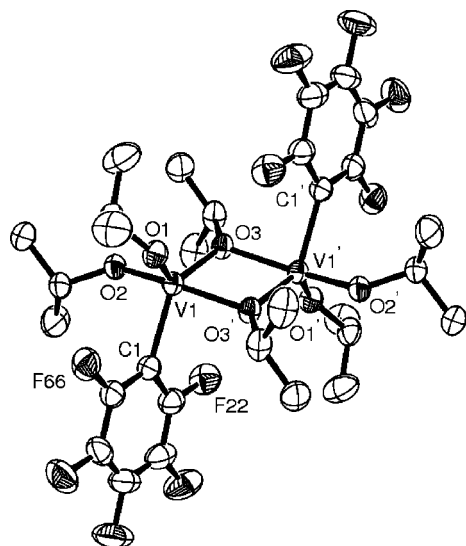


Figure 2. Molecular structure of **2**, showing 50% probability ellipsoids and partial atom-labeling scheme. Hydrogen atoms are omitted for clarity. V(1)–C(1) 2.1127(17), V(1)–O(1) 1.7980(12), V(1)–O(2) 1.7970(13), V(1)–O(3) 1.9220(11), V(1)–O(3)' 2.0276(12), O(3)–V(1)–O(1) 119.91(6), O(3)–V(1)–O(2) 92.54(5), O(1)–V(1)–O(2) 102.88(6), O(1)–V(1)–O(3)' 95.68(6), O(2)–V(1)–O(3)' 161.16(5), O(3)–V(1)–O(3)' 75.14(5), O(1)–V(1)–C(1) 108.03(7), O(2)–V(1)–C(1) 90.84(6), O(3)–V(1)–C(1) 129.71(6), O(3)'–V(1)–C(1) 86.46(6).

five-coordinate distorted square pyramid and a trigonal bipyramid (52% on the Berry pseudorotation path between D_{3h} and C_{4v} , $\tau = 0.52$).²⁶ Terminal and bridged V–O bond distances and angles are in their expected range [ca. 1.71–1.81 Å and 1.92–2.03 Å, respectively] as well as the V–C bond distance [2.1127(18) Å].¹⁶

Reactivity Studies between $Zr(OBu^t)_4$ and $B(C_6F_5)_3$. Similarly, we studied the reactivity of $Zr(OBu^t)_4$ with $B(C_6F_5)_3$. First, an NMR tube reaction of $Zr(OBu^t)_4$ with 1 equiv of $B(C_6F_5)_3$ carried out in CD_2Cl_2 shows that this reaction is not selective, and a mixture of unidentified $-OBu^t$ peaks is observed in the 1H NMR spectrum. ^{19}F and ^{11}B NMR spectra show the presence of the unexpected $[B(C_6F_5)_4]^-$ anion, as well as some $B(OBu^t)(C_6F_5)_2$, the latter being identified by its ^{19}F and ^{11}B NMR spectra by analogy with known analogues $B(OR)(C_6F_5)_2$ ($R = Et$,²⁷ *i*-Pr,²² *n*-Bu²⁸).²⁹ The formation of $B(OBu^t)(C_6F_5)_2$ demonstrates that alkoxide–aryl exchange reaction is not prohibited by steric bulk of the *tert*-butyl group.

In order to isolate a zirconium species, $Zr(OBu^t)_4$ was then reacted with $B(C_6F_5)_3$ in pentane solution (see Scheme 3). The reaction afforded a white precipitate. Several attempts to grow crystals of that compound failed, except when using $CH_3CN-THF$ mixture of solvents. In $CH_3CN-THF$ (10:1), crystals of the trinuclear zirconium salt $[Zr_3(OBu^t)_6(\mu_2-OBu^t)_3(\mu_3-OBu^t)(\mu_3-OCH_2CH_2CH_2CH_3)]^+ [B(C_6F_5)_4]^-$

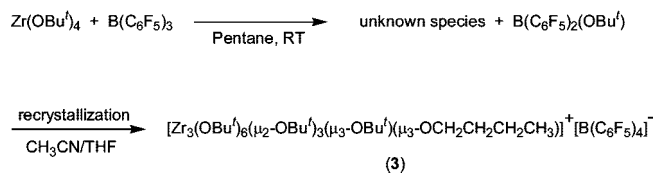
(26) τ is the angular parameter commonly used to describe the geometry around the metal center in pentacoordinate complexes and defined as $\tau = (\alpha - \beta)/60$ (α and β are the two largest L–M–L bond angles, with $\alpha \geq \beta$). Addison, A. W.; Rao, T. N.; Reedijk, J.; van Rijn, J. V. *J. Chem. Soc., Dalton Trans.* **1984**, 1349–1356.

(27) Duchateau, R.; Lancaster, S. J.; Thornton-Pett, M.; Bochmann, M. *Organometallics* **1997**, *16*, 4995–5005.

(28) Parks, D. J.; Piers, W. E.; Yap, G. P. A. *Organometallics* **1998**, *17*, 5492–5503.

(29) Piers et al. reported that diborane $C_6F_4-1,2-[B(C_6F_5)_2]_2$ rapidly abstracts OCH_3^- from $Cp_2Zr(OCH_3)_2$, but the cation in the resulting species is not very stable. Williams, V. C.; Irvine, G. J.; Piers, W. E.; Li, Z.; Collins, S.; Clegg, W.; Elsegood, M. R. J.; Marder, T. B. *Organometallics* **2000**, *19*, 1619–1621.

Scheme 3. Synthesis of Complex 3



$OCH_2CH_2CH_2CH_3][B(C_6F_5)_4]^-$ (**3**) were obtained in low yield and characterized by an X-ray structure determination. Compound **3** crystallized in monoclinic $P2_1/a$ space group, with half a molecule of acetonitrile. The molecular structure of complex **3** is presented in Figure 3 with selected bond distances and angles. Each zirconium atom is surrounded by six oxygen atoms in a distorted octahedral geometry. Overall, the ionic structure results from the coordination of a $\mu_3-O(CH_2)_3CH_3$ group to three metal center units, with loss of two of the 12 initial *tert*-butoxy ligands (as *tert*-butanol) of the three $Zr(OBu^t)_4$. The formation of the $-O(CH_2)_3CH_3$ moiety is explained by ring-opening of a THF molecule (see below). Zr–O bond distances are in the expected range for terminal alkoxide-type ligands (average 1.91–1.92 Å), μ^2 -bridging alkoxide ligands (average 2.17–2.19 Å), and μ_3 -bridging alkoxide ligands (average 2.28–2.35 Å). The three zirconium centers occupy an equilateral triangle, and bridging oxygen atoms are contained in the Zr_3 plane (average Zr–O–Zr 102.18°, O–Zr–O 137.26°, values nearly expected for a planar C_{3v} -distorted regular hexagon). Terminal alkoxides (OBu^t) are nearly situated perpendicular to this plane, and oxygen atoms O(6) and O(8) are in apical location from this plane.

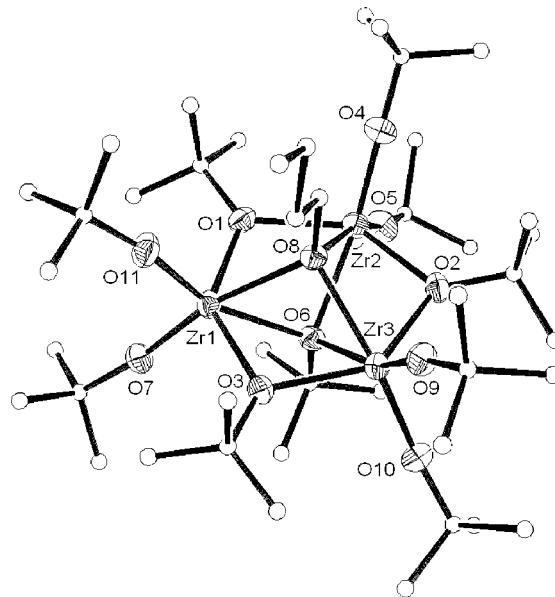


Figure 3. Molecular structure of the cationic part of **3** (the anion $[B(C_6F_5)_4]^-$ and the solvent of crystallization (1/2 CH_3CN) are omitted for clarity), showing 50% probability ellipsoids and partial atom-labeling scheme. Hydrogen atoms are omitted for clarity. O(1)–Zr(2) 2.179(3), O(1)–Zr(1) 2.192(3), O(2)–Zr(2) 2.169(3), O(2)–Zr(3) 2.175(3), O(3)–Zr(1) 2.184(3), O(3)–Zr(3) 2.192(3), O(4)–Zr(2) 1.921(3), O(5)–Zr(2) 1.918(3), O(6)–Zr(2) 2.324(3), O(6)–Zr(1) 2.334(3), O(6)–Zr(3) 2.352(3), O(7)–Zr(1) 1.922(3), O(8)–Zr(1) 2.276(3), O(8)–Zr(3) 2.310(3), O(8)–Zr(2) 2.339(3), O(9)–Zr(3) 1.921(3), O(10)–Zr(3) 1.924(3), O(11)–Zr(1) 1.914(3), Zr(1)···Zr(3) 3.4083(6), Zr(1)···Zr(2) 3.4087(7), Zr(2)···Zr(3) 3.4079(6), O(11)–Zr(1)–O(7) 99.24(13), Zr(2)–O(1)–Zr(1) 102.49(12), Zr(2)–O(6)–Zr(3) 93.58(10), Zr(1)–O(6)–Zr(3) 93.33(10), Zr(1)–O(8)–Zr(3) 95.99(10), Zr(1)–O(8)–Zr(2) 95.21(10), O(11)–Zr(1)–O(1) 99.65(12).

To better understand this reaction, we investigated the reaction of $\text{Zr}(\text{OBU}^t)_4$ and $\text{B}(\text{C}_6\text{F}_5)_3$ by varying the ratio of the reactants and using different solvents (in NMR tube reactions). Nevertheless, we were unable to explain more precisely this reaction and the redox reaction leading to this salt (see Experimental Section). The formation of an intermediate species $[\text{Zr}(\text{OBU}^t)_3(\text{C}_6\text{F}_5)]$ that would react with the borane present in the solution to afford the transient salt $[\text{Zr}(\text{OBU}^t)_3][\text{B}(\text{C}_6\text{F}_5)_4]$ could be envisioned, but the determination of the mechanism of formation of **3** was not elucidated. A titanium compound with a similar structure (with a $[\text{Ti}_3(\text{OPr}^i)_{11}]^+$ core) was recently reported from the reaction of $[\text{Na}][\text{Ti}(\text{OPr}^i)_5]$ with FeCl_3 that affords two different products: the ionic compound $[\text{Ti}_3(\text{OPr}^i)_6(\mu_2\text{-OPr}^i)_3(\mu_3\text{-OPr}^i)_2][\text{FeCl}_4]$ and the mixed oxide–alkoxide iron complex $[\text{Fe}_5\text{Cl}_5(\mu_5\text{-O})(\mu_2\text{-OPr}^i)_8]$.³⁰ The main feature of the cationic zirconium part in **3** is the opening of a THF molecule into a *n*-butoxide group, μ_3 -bonded to the three zirconium atoms, which involves the abstraction of a hydrogen atom from the reaction medium. The THF ring-opening reaction that allows the isolation of **3** may be explained by the presence in solution of the transient cationic species $[\text{Zr}(\text{OBU}^t)_3]^+$, but may also be due to other Lewis acids present in the reaction mixture ($\text{B}(\text{C}_6\text{F}_5)_3$ and $\text{B}(\text{OBU}^t)(\text{C}_6\text{F}_5)_2$).³¹

^1H and ^{13}C NMR spectroscopic data (as well as $^1\text{H}/^1\text{H}$ NOESY and $^1\text{H}/^{13}\text{C}$ HMQC chemical shift correlations) of **3** in $\text{THF-}d_8$ show the peaks attributed to the different terminal and bridged $-\text{OBU}^t$ groups and to the $-\text{OBU}^n$ group (see Experimental Section). Attempts to generate **3** directly from $\text{Zr}(\text{OBU}^t)_4$, $\text{B}(\text{C}_6\text{F}_5)_3$, and the borane adduct $\text{THF}\cdot\text{B}(\text{C}_6\text{F}_5)_3$ in CD_2Cl_2 failed.³² In this case, the ^{11}B NMR spectrum shows mainly the presence of unreacted $\text{THF}\cdot\text{B}(\text{C}_6\text{F}_5)_3$ (δ 3.3 ppm), together with a peak at 38 ppm attributed to $\text{B}(\text{OBU}^t)(\text{C}_6\text{F}_5)_2$ (which demonstrates again that an aryl–alkoxide exchange reaction occurs between the zirconium alkoxide precursor and the borane) and other unattributed minor peaks (δ 23.3, -4.7 , and -13.0 ppm).

During our different attempts to get information on the above reaction, the known³ adduct $\text{THF}\cdot\text{B}(\text{C}_6\text{F}_5)_3$ (**4**) was accidentally obtained as crystals suitable for an X-ray structure determination. The molecular structure of **4** is presented in Figure 4. The B–O bond distance of 1.5847(18) Å has to be compared to that of the related $\text{THF}\cdot\text{B}(\text{C}_6\text{H}_5)_3$ (1.6500(17) Å)³³ and to $\text{Mes}_2\text{P}-\text{C}_6\text{F}_4-\text{B}(\text{C}_6\text{F}_5)_2\cdot\text{THF}$ (1.625 Å),³⁴ reflecting again the stronger Lewis acidity of $\text{B}(\text{C}_6\text{F}_5)_3$.

In an other attempt to probe this reaction, but now using 2 or 3 equiv of $\text{Zr}(\text{OBU}^t)_4$ and 1 equiv of $\text{B}(\text{C}_6\text{F}_5)_3$ and in pentane solution, we obtained a white precipitate. As above, the precipitate was isolated by filtration and analyzed by ^{19}F and ^1H NMR spectroscopy, showing again the characteristic peaks of the $[\text{B}(\text{C}_6\text{F}_5)_4]^-$ anion and a broad signal in the range 1.30–1.90 ppm attributed to different Zr–OBU^t species. The

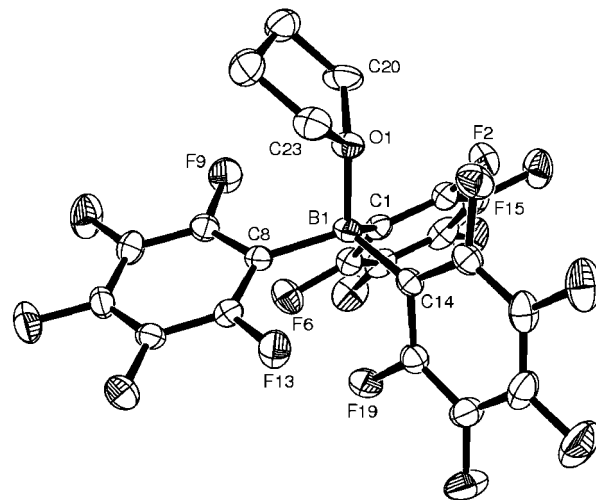


Figure 4. Molecular structure of **4**, showing 50% probability ellipsoids and partial atom-labeling scheme. Hydrogen atoms are omitted for clarity. B(1)–O(1) 1.5848(18), B(1)–C(14) 1.631(2), B(1)–C(1) 1.637(2), B(1)–C(8) 1.645(2), O(1)–B(1)–C(14) 108.89(11), O(1)–B(1)–C(1) 107.96(11), O(1)–B(1)–C(8) 104.60(11), C(14)–B(1)–C(1) 105.26(11), C(14)–B(1)–C(8) 114.25(11), C(1)–B(1)–C(8) 115.65(11).

filtrate, after evaporation to dryness, gave a pale yellow solid, which was analyzed by NMR spectroscopy in CD_2Cl_2 (^1H , ^{19}F , and ^{11}B) as being a mixture of $\text{B}(\text{OBU}^t)(\text{C}_6\text{F}_5)_2$ and other Zr–OBU^t peaks in the range 1.2–1.8 ppm. However, addition of CH_3CN to this solid caused evolution of H_2 gas and formation in the NMR tube of a few yellow crystals of a new complex, **5**. This compound was unambiguously characterized by an X-ray structure analysis as being the tetrametallic neutral complex $[\text{Zr}_2(\text{OBU}^t)_5(\mu\text{-OBU}^t)_2(\mu\text{-}N,N'\text{-N}(\text{H})\text{C}(\text{CH}_3)=\text{C}(\text{H})\text{C}\equiv\text{N})_2]$ (**5**). Salient structural features for the zirconium complex **5** are depicted in Figure 5, with selected bond distances and angles.

The crystal structure of **5** revealed a tetrametallic compound composed of two dimeric $[\text{Zr}_2(\text{OBU}^t)_5(\mu\text{-OBU}^t)_2]$ units held together by two $\mu\text{-}N,N'\text{-N}(\text{H})\text{C}(\text{CH}_3)=\text{C}(\text{H})\text{C}\equiv\text{N}$ moieties. Dimerization of CH_3CN molecules through C,C coupling occurred to form the organic crotonylamido linker. The crotonylamido arrangement, also obtained by activation and dimerization of acetonitrile, was recently reported by us for zirconium chemistry (starting from Cp_2ZrPh_2 , CH_3CN , and $\text{B}(\text{C}_6\text{F}_5)_3$)¹² and by Teuben for yttrium chemistry.³⁵ Zr–O bond lengths are found in the expected range (ca. 1.91–1.95 Å), and the crotonylamido linker has similar bond lengths and angles to those found in the above-mentioned zirconocene and yttrium complexes. At one side of the crotonylamido ligand, the nitrogen atom [N(1)-H] of an imine functionality [the CN bond distance is in agreement with a double bond: C(9)=N(1) 1.349(3) Å] is bridging two distorted octahedral zirconium centers [Zr(1)–N(1) 2.413(2) Å, Zr(2)–N(1) 2.404(2) Å]. The second side of the ligand contains a nitrile skeleton by which it is coordinated to the zirconium center [Zr(2')] of a symmetry-related dimeric unit [Zr(2')–N(2') 2.306(2) Å]. The C≡N bond distance of 1.154(3) Å is consistent with a triple-bond character associated with a nearly linear N(2)–C(33)–C(10) angle (175.0(3)°). As a result, this crotonylamido fragment can be considered as a donor ligand to the dimer form of $\text{Zr}(\text{OBU}^t)_4$.

Although fortuitous, the issue of this reaction was confirmed by the characterization of a few crystals of **5** (with identical

(30) Reis, D. M.; Nunes, G. G.; Sa, E. L.; Friedermann, G. R.; Mangrich, A. S.; Evans, D. J.; Hitchcock, P. B.; Leigh, G. J.; Soares, J. F. *New J. Chem.* **2004**, *28*, 1168–1176.

(31) For selected examples of THF-ring-opening mediated by Lewis acidic metal centers or main-group Lewis acids, see: (a) Guo, Z.-Y.; Bradley, P. K.; Jordan, R. F. *Organometallics* **1992**, *11*, 2690–2693. (b) Boisson, C.; Berthet, J. C.; Lance, M.; Nierlich, M.; Ephritikhine, M. *Chem. Commun.* **1996**, 2129–2130. (c) Borkowsky, S. L.; Jordan, R. F.; Hinch, G. D. *Organometallics* **1991**, *10*, 1268–1274. (d) Welch, G. C.; Masuda, J. D.; Stephan, D. W. *Inorg. Chem.* **2006**, *45*, 478–480.

(32) This experiment suggests that the solvent is the source of proton in the reaction conducted in THF.

(33) Niehues, M.; Erker, G.; Meyer, O.; Fröhlich, R. *Organometallics* **2000**, *19*, 2813–2815.

(34) Welch, G. C.; Juan, R. R. S.; Masuda, J. D.; Stephan, D. W. *Science* **2006**, *314*, 1124–1126.

(35) Duchateau, R.; Tuinstra, T.; Brussee, E. A. C.; Meetsma, A.; van Duijnen, P. T.; Teuben, J. H. *Organometallics* **1997**, *16*, 3511–3522.

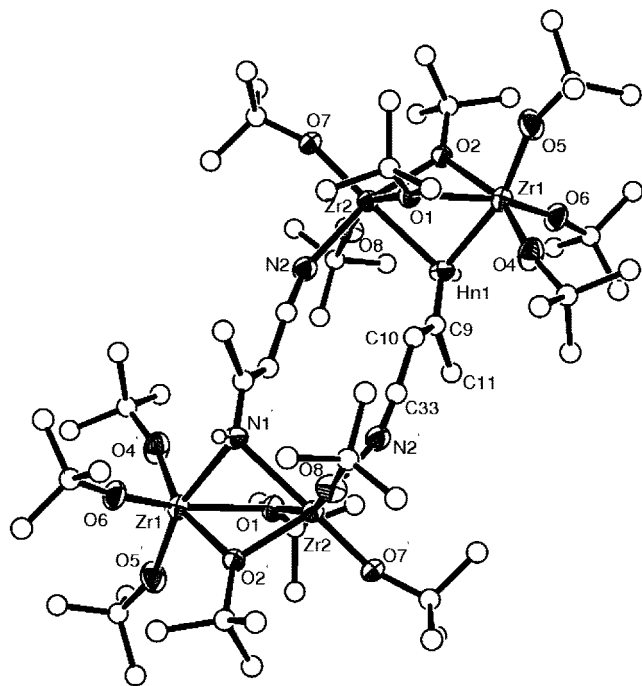


Figure 5. Molecular structure of **5**, showing 50% probability ellipsoids and partial atom-labeling scheme. Hydrogen atoms are omitted for clarity. C(9)–N(1) 1.349(3), C(9)–C(10) 1.354(4), C(9)–C(11) 1.514(4), C(10)–C(33) 1.392(4), C(33)–N(2) 1.154(3), O(1)–Zr(2) 2.1832(18), O(1)–Zr(1) 2.2817(18), O(2)–Zr(2) 2.0852(18), O(2)–Zr(1) 2.3353(18), N(1)–Zr(2) 2.404(2), N(1)–Zr(1) 2.413(2), O(4)–Zr(1) 1.932(2), O(5)–Zr(1) 1.947(2), O(6)–Zr(1) 1.9449(19), O(7)–Zr(2) 1.9233(18), O(8)–Zr(2) 1.9168(19), N(2)–Zr(2) 2.306(2), N(1)–C(9)–C(10) 121.7(3), N(1)–C(9)–C(11) 118.2(3), C(10)–C(9)–C(11) 120.1(3), C(9)–C(10)–C(33) 122.7(3), N(2)–C(33)–C(10) 175.0(3), Zr(2)–O(1)–Zr(1) 95.92(7), Zr(2)–O(2)–Zr(1) 97.07(7), C(9)–N(1)–Zr(2) 124.19(18), C(9)–N(1)–Zr(1) 123.84(19), Zr(2)–N(1)–Zr(1) 87.02(7), C(33)–N(2)–Zr(2) 161.3(2), O(4)–Zr(1)–O(6) 97.82(9), O(4)–Zr(1)–O(5) 102.00(10), O(6)–Zr(1)–O(5) 102.13(9), O(4)–Zr(1)–O(1) 94.73(8), O(6)–Zr(1)–O(1) 153.31(8), O(5)–Zr(1)–O(1) 98.13(8), O(4)–Zr(1)–O(2) 160.39(8), O(6)–Zr(1)–O(2) 90.75(8), O(5)–Zr(1)–O(2) 93.33(8), O(1)–Zr(1)–O(2) 70.78(6), O(4)–Zr(1)–N(1) 92.09(9), O(6)–Zr(1)–N(1) 86.01(8), O(5)–Zr(1)–N(1) 162.47(9), O(1)–Zr(1)–N(1) 70.04(7), O(2)–Zr(1)–N(1) 70.84(7), O(8)–Zr(2)–N(2) 85.62(8), O(7)–Zr(2)–N(2) 89.99(8), O(2)–Zr(2)–N(2) 162.24(8), O(1)–Zr(2)–N(2) 90.46(8), O(8)–Zr(2)–N(1) 87.77(9), O(7)–Zr(2)–N(1) 171.88(8), O(2)–Zr(2)–N(1) 75.28(7), O(1)–Zr(2)–N(1) 71.83(7), N(2)–Zr(2)–N(1) 88.62(8).

cell parameters) from several experiments. The formation of the minor byproduct **5** remains unclear and probably results from a complex cascade of reactions.

In the course of our investigations, we noticed that liquid $Zr(OBu^t)_4$ was insoluble in acetonitrile. However, adding a few drops of dichloromethane to liquid $Zr(OBu^t)_4$, followed by addition of CH_3CN , afforded a gel, from which we were able to obtain crystals of the μ -acetonitrile adduct of the dimeric zirconate $[Zr(OBu^t)_3(\mu-OBu^t)]_2(\mu-N\equiv CCH_3)$ (**6**). The structure of **6** (see Figure 6) is briefly described below, as it is related to the structure of compound **5** and because no molecular structure is known for “ $Zr(OBu^t)_4$ ”. It is important to note that compound **6** could not be isolated because the acetonitrile ligand is removed during the vacuum drying step, giving back $Zr(OBu^t)_4$. In the solid state, **6** is a dimeric complex composed of two $Zr(OBu^t)_3$ units linked by two bridging $-OBu^t$ ligands and one N atom of a CH_3CN donor. The coordination geometry of the zirconium

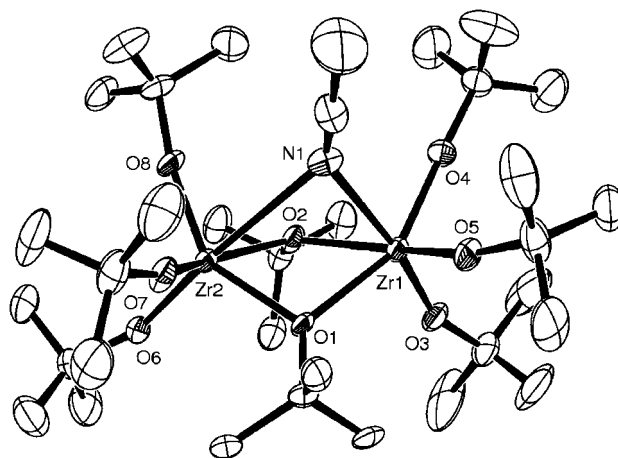


Figure 6. Molecular structure of **6**, showing 50% probability ellipsoids and partial atom-labeling scheme. Hydrogen atoms are omitted for clarity. C(33)–N(1) 1.243(5), N(1)–Zr(1) 2.649(3), O(1)–Zr(2) 1.9662(18), O(1)–Zr(1) 2.215(2), O(2)–Zr(1) 2.1496(19), O(2)–Zr(2) 2.2618(19), O(3)–Zr(1) 1.959(2), O(4)–Zr(1) 1.924(2), O(5)–Zr(1) 2.037(2), O(6)–Zr(2) 2.072(2), O(7)–Zr(2) 2.074(2), O(8)–Zr(2) 1.765(2), Zr(1)···Zr(2) 0.3.2902(4) N(1)–C(33)–C(34) 179.5(5), Zr(2)–O(1)–Zr(1) 103.62(8), Zr(1)–O(2)–Zr(2) 96.43(8).

centers is a six-coordinate distorted octahedron. Terminal Zr–O bond distances span over 1.76–2.07 Å, whereas bridged Zr–O bond distances are naturally longer [ca. 1.96–2.26 Å]. The Zr–N bond distances amount to 2.649(3) and 2.886(3) Å.

In a last attempt of getting crystals of hypothetical transient species $[Zr(OBu^t)_3(C_6F_5)]$ and $[Zr(OBu^t)_3][B(C_6F_5)_4]$ from a reaction mixture composed of $Zr(OBu^t)_4$ and $B(C_6F_5)_3$, but now in CH_2Cl_2 –pentane solutions, and due to the presence of adventitious water during the crystallization process (that lasted one month at RT and certainly resulted in hydrolysis of $B(C_6F_5)_3$ into $HOB(C_6F_5)_2$, see below), we obtained crystals of a new compound (**7**). An X-ray crystallographic study of **7** reveals it to be an unprecedented dimeric complex formulated as $[Zr(OBu^t)_2\{\mu-O-OB(OBu^t)(C_6F_5)_2-\kappa^2-O,O\}]_2$ (see Figure 7).

The rather unusual $OB(OBu^t)$ bonding mode in **7** prompted us to prepare this compound in a more direct route. Thus, **7** was prepared more conveniently and in higher yield by the direct reaction of $Zr(OBu^t)_4$ and $(HO)B(C_6F_5)_2$ (Scheme 5). However, this reaction was not clean, as we also observed signals corresponding to $B(OBu^t)(C_6F_5)_2$. This could suggest the formation of an intermediate $[Zr-OH]$ species.³⁶

Zirconium centers in complex **7** show a five-coordinate, very distorted geometry (that is probably best described as a tetrahedron with the fourth ligand being a chelating $\{OB(OBu^t)(C_6F_5)_2-\kappa^2-O,O\}$ ligand). Within this new dianionic entity $\{OB(OBu^t)(C_6F_5)_2-\kappa^2-O,O\}$, it is interesting to note the formation of an interaction between the oxygen of a *tert*-butoxide group attached to the zirconium atom and the boron atom, the corresponding B–O bond [B(1)–O(1) 1.533(4) Å] being slightly longer than the B–O bond formed with the bridging oxygen [B(1)–O(2) 1.480(4) Å]. This could suggest that the B(1)–O(1) bond is better regarded as a dative bond, rather than a covalent bond. A dative B–O bond is also more likely according to ¹¹B NMR spectroscopy of **7** ($\delta = +5.0$ ppm). To our knowledge, this type of interaction between an alkoxide

(36) For a review on hydrolysis of metal alkoxides, see: Brinker, C. J.; Scherer, G. W. In *Sol-Gel Science, The Physics and Chemistry of Sol-Gel Processing*; Academic Press: New York, 1990.

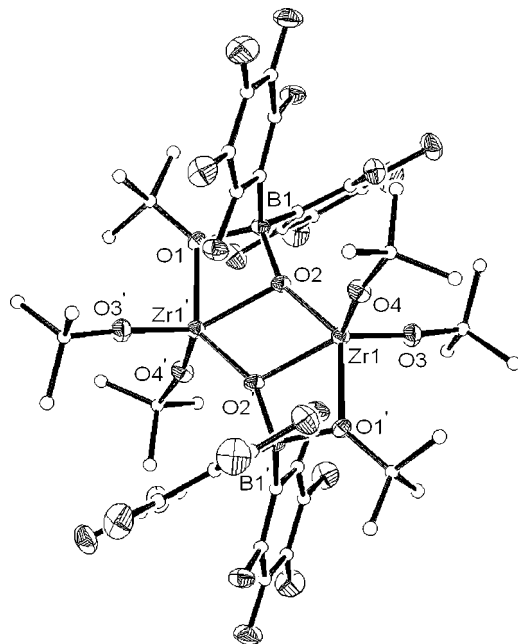
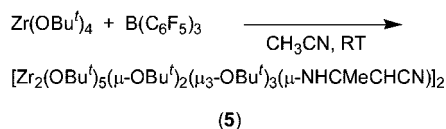
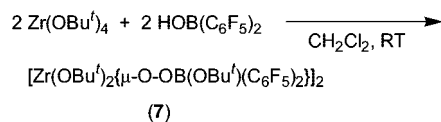


Figure 7. Molecular structure of **7**, showing 50% probability ellipsoids and partial atom-labeling scheme. Hydrogen atoms are omitted for clarity. C(1)–B(1) 1.633(4), C(7)–B(1) 1.658(5), O(1)–B(1) 1.533(4), O(1)–Zr(1) 2.186(2), O(2)–B(1) 1.480(4), O(2)–Zr(1) 2.068(2), O(2)–Zr(1) 2.208(2), O(4)–Zr(1) 1.885(2), O(3)–Zr(1) 1.909(2), B(1)–O(1)–Zr(1) 97.98(16), B(1)–O(2)–Zr(1) 151.30(19), B(1)–O(2)–Zr(1) 98.76(17), Zr(1)–O(2)–Zr(1) 106.67(8), O(4)–Zr(1)–O(3) 104.62(10), O(4)–Zr(1)–O(2) 103.45(9), O(3)–Zr(1)–O(2) 107.48(9), O(4)–Zr(1)–O(1) 101.37(9), O(3)–Zr(1)–O(1) 100.90(9), O(2)–Zr(1)–O(1) 135.69(8), O(4)–Zr(1)–O(2) 113.77(9), O(3)–Zr(1)–O(2) 140.41(9), O(2)–Zr(1)–O(2) 73.33(8), O(1)–Zr(1)–O(2) 63.18(8), O(2)–B(1)–O(1) 99.6(2), O(2)–B(1)–C(1) 107.6(2), O(1)–B(1)–C(1) 114.3(3), O(2)–B(1)–C(7) 111.0(2), O(1)–B(1)–C(7) 105.6(2).

Scheme 4. Synthesis of Complex 5



Scheme 5. Synthesis of Complex 7



ligand and a boron-containing ligand is unknown. The Zr–O bond distances of the dissymmetric bridge are 2.068(2) Å (Zr(1)–O(2)) and 2.208(2) Å (Zr(1)–O(2)'), while the alkoxide Zr–O bond distances are in the normal range (1.89–1.91 Å).

Consistent with the solid-state structure, the ^1H NMR data of **7** in CD_2Cl_2 exhibit two signals for the two types of *O**t*-Bu groups (terminal and bridged alkoxy groups). Furthermore, the ^{19}F NMR spectrum presents broad C_6F_5 signals for *o*-, *p*-, and *m*-F atoms, indicative of a dynamical behavior of the C_6F_5 ligand.³⁷ A dative $\text{Zr}\cdots\text{o-F}$ interaction is suggested in room-temperature solution. Further studies on this interesting new ligand bonding mode will be needed to clarify this point.

Conclusions

We have demonstrated the reactivity of the borane $\text{B}(\text{C}_6\text{F}_5)_3$ with simple group 4 and 5 metal alkoxides. The reactions of $\text{Ti}(\text{O}i\text{Pr})_4$ and $\text{V}(\text{O}i\text{Pr})_4$ with 1 equiv of $\text{B}(\text{C}_6\text{F}_5)_3$ in pentane at room temperature yielded dimeric organometallic complexes **1** and **2**. Their formation can be regarded as an alkoxide–aryl exchange reaction between $[\text{M-O}i\text{Pr}]$ ($\text{M} = \text{Ti}, \text{V}$) and $\text{B}(\text{C}_6\text{F}_5)_3$, from the elusive zwitterionic $[\text{M}(\text{O}i\text{Pr})_3(\mu\text{-O}i\text{Pr})(\text{B}(\text{C}_6\text{F}_5)_3)]$ or ionic $[\text{M}(\text{O}i\text{Pr})_3][\text{B}(\text{O}i\text{Pr})(\text{C}_6\text{F}_5)_3]$ intermediate (that could not be isolated). The reaction of $\text{Zr}(\text{O}t\text{Bu})_4$ and $\text{B}(\text{C}_6\text{F}_5)_3$ proceeds differently with formation of more complex products due to further reaction with solvents (THF, acetonitrile). The formation of **3** is the result of a more complex reaction, as demonstrated by the presence of the $[\text{B}(\text{C}_6\text{F}_5)_4]^-$ anion. The sterically crowded *tert*-butoxide ligand could prevent the formation of a dimeric species analogous to **1** or **2**, leaving a transient species ($[\text{Zr}(\text{O}t\text{Bu})_3(\text{C}_6\text{F}_5)]$ or $[\text{Zr}(\text{O}t\text{Bu})_3][\text{B}(\text{C}_6\text{F}_5)_4]$) able to react with the zirconate and the borane still present in the solution, thus affording the polymetallic cationic zirconium alkoxide **3**, with an additional *n*-butoxide ligand due to ring-opening reaction of THF. In acetonitrile, another unexpected tetrametallic complex (**4**) was obtained that results from the dimerization of acetonitrile molecules and coordination to dimers of $\text{Zr}(\text{O}t\text{Bu})_4$. Finally, we could observe the formation of a new ligand bonding mode in the reaction of $\text{Zr}(\text{O}t\text{Bu})_4$ with the boronic acid $(\text{HO})\text{B}(\text{C}_6\text{F}_5)_2$, which leads to unprecedented complex **7**. Future work will focus on the isolation of stable zwitterionic or cationic species generated during M-OR activation with $\text{B}(\text{C}_6\text{F}_5)_3$, using additional ancillary ligands.

Experimental Section

General Methods and Instrumentation. All manipulations were carried out using standard Schlenk line or drybox techniques under an atmosphere of argon. Solvents were refluxed and dried over appropriate drying agents under an atmosphere of argon, collected by distillation, and stored in a drybox over activated 4 Å molecular sieves. Deuterated solvents were degassed and dried over activated 4 Å molecular sieves. NMR spectra were recorded on Bruker AC 200, AM 250, AMX 400, Avance 400, and Avance 500 spectrometers, were referenced internally to residual protio-solvent (^1H) resonances, and are reported relative to tetramethylsilane ($\delta = 0$ ppm). ^{19}F NMR spectra were recorded on a Bruker AC 200 (188.298 MHz) or Avance 400 spectrometer (376.441 MHz) and referenced to CFCl_3 . ^{11}B NMR (128.37 MHz; reference $\text{BF}_3 \cdot \text{Et}_2\text{O}$) spectra were recorded on a Bruker AMX 400 spectrometer. Chemical shifts are quoted in δ (ppm). Multiplicities and peak types are abbreviated: singlet, s; doublet, d; triplet, t; broad, br; Cq, quaternary carbon. Infrared spectra were prepared as KBr pellets under argon in a glovebox and were recorded on a Perkin-Elmer Spectrum GX FT-IR spectrometer. Infrared data are quoted in wavenumber (cm^{-1}). EPR spectra were obtained by using a Bruker ESP300E spectrometer. Magnetic susceptibilities were determined by Faraday's method. Elemental analyses (C, H, N) were performed at the Laboratoire de Chimie de Coordination (Toulouse, France). $\text{Ti}(\text{O}i\text{-Pr})_4$ and $\text{Zr}(\text{O}t\text{-Bu})_4$ were purchased from Aldrich Inc. or Strem Inc. and used after distillation under reduced pressure. $\text{V}(\text{O}i\text{-}$

(37) For selected Zr–F interactions, see ref 12 and: (a) Pintado, G. J.; Thornton-Pett, M.; Bouwkamp, M.; Meetsma, A.; Hessen, B.; Bochmann, M. *Angew. Chem., Int. Ed. Engl.* **1997**, *36*, 2358–3831. (b) Pintado, G. J.; Lancaster, S. J.; Thornton-Pett, M.; Bochmann, M. *J. Am. Chem. Soc.* **1998**, *120*, 6816–6817. (c) Siedle, A. R.; Newmark, R. A.; Lamanna, W. N.; Huffman, J. C. *Organometallics* **1993**, *12*, 1491–1492. (d) Hannig, F.; Fröhlich, R.; Bergander, K.; Erker, G.; Petersen, J. L. *Organometallics* **2004**, *23*, 4495–4502.

Table 1. Crystallographic Data, Data Collection, and Refinement Parameters for Compounds 1–7

	1	2	3	4	5	6	7
chemical formula	C ₃₀ H ₄₂ F ₁₀ O ₆ Ti ₂	C ₃₀ H ₄₂ F ₁₀ O ₆ V ₂	C ₁₃₈ H ₂₀₁ B ₂ F ₂₀ O ₂₂ NZr ₆	C ₂₂ H ₈ BF ₁₅ O	C ₆₄ H ₁₃₆ N ₄ O ₁₄ Zr ₄	C ₃₄ H ₇₅ NO ₈ Zr ₂	C ₄₈ H ₅₄ B ₂ F ₂₀ O ₈ Zr ₂
fw	784.38	790.52	3551.91	584.09	1550.65	808.39	1342.97
cryst syst	monoclinic	triclinic	monoclinic	monoclinic	monoclinic	orthorhombic	triclinic
space group	<i>P</i> 2 ₁ / <i>n</i>	<i>P</i> $\bar{1}$	<i>P</i> 2 ₁ / <i>a</i>	<i>P</i> 2 ₁ / <i>n</i>	<i>P</i> 2 ₁ / <i>n</i>	<i>Pbca</i>	<i>P</i> $\bar{1}$
<i>a</i> , Å	8.9690(7)	9.4241(11)	20.2421(15)	14.2611(13)	14.1142(5)	17.1407(5)	10.872(2)
<i>b</i> , Å	16.8220(14)	9.5143(12)	20.2310(15)	11.2276(8)	15.6865(5)	19.1840(6)	11.866(3)
<i>c</i> , Å	12.0463(10)	11.2825	21.0455(17)	14.7056(12)	18.9583(6)	26.3148(8)	12.017(3)
α , deg	90	75.416(15)	90	90	90	90	110.37(2)
β , deg	96.564(7)	67.418(14)	112.960(8)	115.967(9)	103.676(4)	90	105.386(18)
γ , deg	90	78.047(15)	90	90	90	90	98.153(18)
<i>V</i> , Å ³	1805.6(3)	897.05(19)	7935.7(11)	2116.9(3)	4078.4(2)	8653.0(5)	1353.3(5)
<i>Z</i>	2	2	2	4	2	8	1
<i>D</i> _{calc} , g cm ⁻³	1.443	1.463	1.486	1.833	1.263	1.241	1.648
μ (Mo K α), mm ⁻¹	0.532	0.611	0.487	0.202	0.551	0.523	0.505
<i>F</i> (000)	808	406	3638	1152	1640	3440	676
θ range (deg)	3.23 to 30.54	2.50 to 26.15	2.69 to 26.37	3.08 to 32.06	2.69 to 32.10	2.55 to 28.28	3.20 to 24.71
measd reflns	16 234	8723	57 500	21 453	43 674	74 061	8990
no. of unique reflns/Rint	5078/0.0466	3220/0.0352	16205/0.0779	7006/0.0298	13 539/0.0464	10 703/0.0479	4593/0.0460
no. of params/restraints	223/0	223/0	986/2	352/0	413/1	431/0	370/0
final <i>R</i> indices all data	R1 = 0.0706, wR2 = 0.0957	R1 = 0.0355, wR2 = 0.0920	R1 = 0.1111, wR2 = 0.1191	R1 = 0.0877, wR2 = 0.0971	R1 = 0.0916, wR2 = 0.1330	R1 = 0.0728, wR2 = 0.1272	R1 = 0.0488, wR2 = 0.1023
final <i>R</i> indices [<i>I</i> > σ (2) <i>I</i>]	R1 = 0.0390, wR2 = 0.0862	R1 = 0.0335, wR2 = 0.0904	R1 = 0.0474, wR2 = 0.1018	R1 = 0.0396, wR2 = 0.084	R1 = 0.0370, wR2 = 0.0948	R1 = 0.0357, wR2 = 0.0939	R1 = 0.0404, wR2 = 0.0973
goodness of fit	0.928	1.062	0.869	0.860	1.081	1.162	1.013
$\Delta\rho_{\max}$, $\Delta\rho_{\min}$	0.402 and -0.327	0.244 and -0.321	0.603 and -0.603	0.256 and -0.217	0.842 and -0.694	0.918 and -0.630	0.819 and -0.814

Pr)₄,³⁸ B(C₆F₅)₃,^{39,40} and (HO)B(C₆F₅)₂^{41,42} were prepared according to literature procedures.

Crystal Structure Determination. Crystal data collection and processing parameters are given in Table 1. Crystals of **1** (colorless blocks), **2** (brown-red blocks), **3** (colorless plates), **4** (colorless blocks), **5** (colorless blocks), **6** (colorless blocks), and **7** (colorless blocks) were obtained. The selected crystals, sensitive to air and moisture, were mounted on a glass fiber using perfluoropolyether oil and cooled rapidly to 180 K in a stream of cold N₂. For all the structures, data were collected at low temperature (*T* = 180 K) on a Stoe imaging plate diffraction system (IPDS), equipped with an Oxford Cryosystems Cryostream cooler device or an Oxford Diffraction Kappa CCD Excalibur diffractometer equipped with an a cryojet from Oxford Instruments and using graphite-monochromated Mo K α radiation (λ = 0.71073 Å). Final unit cell parameters were obtained by means of a least-squares refinement of a set of 8000 well-measured reflections, and crystal decay was monitored during data collection by measuring 200 reflections by image; no significant fluctuation of intensities has been observed. Structures have been solved by means of direct methods using the program SIR92⁴³ and subsequent difference Fourier maps, models were refined by least-squares procedures on *F*² by using SHELXL-97⁴⁴ integrated in the package WINGX version 1.64,⁴⁵ and empirical absorption corrections were applied to the data.⁴⁶ Details of the structure solution and refinements are given in the Supporting Information (CIF file). A full listing of atomic coordinates, bond lengths and angles, and displacement parameters for all structures has been deposited at the Cambridge Crystallographic Data Centre.

[Ti(OPr^{*t*})₂(μ -OPr^{*t*})(C₆F₅)₂ (1). A solution of B(C₆F₅)₃ (281 mg, 0.55 mmol) in pentane (4 mL) was added dropwise to a solution of [Ti(OPr^{*t*})₄] (200 mg, 0.55 mmol) in pentane (3 mL) at room

temperature. The reaction mixture was stirred for 2 h at room temperature and then cooled in the freezer (-18 °C) overnight. Red crystals were filtered off, washed with pentane, and dried under vacuum (152 mg, 64%). ¹H NMR (C₆D₆): δ 4.60 (br m, 1H, CH), 1.16 (d, *J* = 6.1 Hz, 3H, CH₃). ¹⁹F NMR (C₆D₆): δ -119.7 (d, *o*-F, C₆F₅), -157.3 (t, *p*-F, C₆F₅), -162.2 (br s, *m*-F, C₆F₅). Anal. Calc for C₁₅H₂₁F₅O₃Ti: C, 45.94; H, 5.40. Found: C, 45.50; H, 5.32.

The ¹H, ¹⁹F, and ¹¹B NMR (C₆D₆) data of the filtrate (after workup) showed signals corresponding to [B(OPr^{*t*})(C₆F₅)₂] (¹H NMR: δ 4.13 (sept, *J* = 6.0 Hz, 1H, CH), 1.07 (d, *J* = 6.0 Hz, 1H, CH₃). ¹⁹F NMR δ -132.8, -149.2, -160.8. ¹¹B NMR: δ 39.7).

[V(OPr^{*t*})₂(μ -OPr^{*t*})(C₆F₅)₂ (2). A suspension of B(C₆F₅)₃ (281 mg, 0.35 mmol) in pentane (4 mL) was added dropwise to a blue solution of [V(OPr^{*t*})₄] (100 mg, 0.35 mmol) in pentane (3 mL) at room temperature, causing an immediate color change to brown. The reaction mixture was stirred for 2 h at room temperature and then left 2 weeks at RT. Brown crystals were filtered off, washed with cold pentane, and dried under vacuum (94 mg, 68%). EPR (toluene, RT): *g* = 1.974; *a*(⁵¹V) 54.1 G. μ_{eff} = 2.44 μ_{B} (per dimer). ⁵¹V NMR (C₆D₆): δ -554 (*w*_{1/2} = 260 Hz). Anal. Calc for C₁₅H₂₁F₅O₃V: C, 45.58; H, 5.36. Found: C, 45.41; H, 5.15.

The ¹H, ¹⁹F, and ¹¹B NMR (C₆D₆) data of the filtrate (after workup) showed signals corresponding to [B(OPr^{*t*})(C₆F₅)₂] (see synthesis of **1**). This reaction was monitored by means of EPR (in a sealed capillary tube, in pentane and in toluene solutions) and NMR (¹H, ¹⁹F, ¹¹B, ⁵¹V, in C₆D₆) spectroscopic analyses, which proved the reaction to proceed through an EPR-silent, red intermediate species **I**. ¹H NMR (C₆D₆): δ 4.86 (br m, 3H, CH), 4.30 (sept, *J* = 6.0 Hz, 1H, CH_{bridged}), 1.09 (d, *J* = 6.0 Hz, 3H, CH_{3bridged}), 0.87 (d, *J* = 6.1 Hz, 3H, CH₃). ¹⁹F NMR (C₆D₆): δ -131.2 (br s, *o*-F, C₆F₅), -157.8 (s, *p*-F, C₆F₅), -164.4 (br s, *m*-F, C₆F₅). ¹¹B NMR (C₆D₆): δ -5.0. ⁵¹V NMR (C₆D₆): δ -742 (*w*_{1/2} = 15 Hz).

[Zr₃(OBu^{*t*})₆(μ ₂-OBu^{*t*})₃(μ ₃-OBu^{*t*})(μ ₃-OCH₂CH₂CH₂CH₃)] [B(C₆F₅)₄], (CH₃CN)_{0.5}(3**).** A solution of B(C₆F₅)₃ (120 mg, 0.23 mmol) in pentane (6 mL) was added dropwise to a solution of [Zr(OBu^{*t*})₄] (90 mg, 0.23 mmol) in pentane (5 mL) at room temperature. The white precipitate obtained was filtered off and washed with pentane (yield 110 mg). In THF-*d*₈ the ¹H NMR showed the characteristic peaks of **3** (see below) with two other -OBu^{*t*} groups (one at 1.41 ppm related to B(OBu^{*t*})(C₆F₅)₂ and a second unattributed peak at 1.27 ppm; for comparison the ¹H NMR spectrum of [Zr(OBu^{*t*})₄] in THF-*d*₈ shows a peak at 1.37 ppm). Dissolution of the precipitate in CH₃CN and THF (10:1) allowed the formation of microcrystals of **3**. Yield: 32 mg (23% based on Zr).

(38) Bradley, D. C.; Mehta, L. M. *Can. J. Chem.* **1962**, *40*, 1183–1188.

(39) Massey, A. G.; Park, A. J. *J. Organomet. Chem.* **1964**, *2*, 245–250.

(40) Massey, A. G.; Park, A. J. *J. Organomet. Chem.* **1966**, *5*, 218–225.

(41) Chambers, R. D.; Chivers, T. *J. Chem. Soc.* **1965**, 3933–3939.

(42) Beringhelli, T.; D'Alfonso, G.; Donghi, D.; Maggioni, D.; Mercandelli, D.; Sironi, A. *Organometallics* **2003**, *22*, 1588–1590.

(43) Altomare, A.; Cascarano, G.; Giacovazzo, G.; Guagliardi, A.; Burla, M. C.; Polidori, G.; Camalli, M. *J. Appl. Crystallogr.* **1994**, *27*, 435.

(44) Sheldrick, G. M. *SHELX97 [Includes SHELXS97, SHELXL97, CIFTAB]—Programs for Crystal Structure Analysis (Release 97-2)*; Institut für Anorganische Chemie der Universität: Göttingen, Germany, 1998.

(45) Farrugia, L. J. *J. Appl. Crystallogr.* **1999**, *32*, 837–838.

(46) Walker, N.; Stuart, D. *Acta Crystallogr. A* **1983**, *39*, 158–166.

^1H NMR (THF- d_8): δ 4.13 (AA'B system, app. $J = 17.6$ Hz, $\text{OCH}_2\text{CH}_2\text{CH}_2\text{CH}_3$), 2.51 (m, $\text{OCH}_2\text{CH}_2\text{CH}_2\text{CH}_3$), 2.10 (s, 9H, μ_3 -*Ot*-Bu), 2.07 (s, 3H, CH_3CN), 1.90 (s, 27 H, μ_2 -*Ot*-Bu), 1.70 (s, 27 H, *Ot*-Bu terminal), 1.65 (s, 27 H, *Ot*-Bu terminal), 1.38 (m, 2H, $\text{OCH}_2\text{CH}_2\text{CH}_2\text{CH}_3$), 1.15 (t, $J = 14.7$ Hz 2H, $\text{OCH}_2\text{CH}_2\text{CH}_2\text{CH}_3$). ^{13}C NMR (THF- d_8): δ 71.88 ($\text{OCH}_2\text{CH}_2\text{CH}_2\text{CH}_3$), 33.69 ($\text{OCH}_2\text{CH}_2\text{CH}_2\text{CH}_3$), 33.57 (μ_2 -*Ot*-Bu), 32.24 (*Ot*-Bu terminal), 32.15 (*Ot*-Bu terminal), 31.70 (μ_3 -*Ot*-Bu), 17.89 ($\text{OCH}_2\text{CH}_2\text{CH}_2\text{CH}_3$), 12.64 ($\text{OCH}_2\text{CH}_2\text{CH}_2\text{CH}_3$), 0.34 (CH_3CN). ^{11}B NMR (THF- d_8): δ -16.9. ^{19}F NMR (THF- d_8): δ -133.0 (d, *o*-F, C_6F_5), -165.2 (t, *p*-F, C_6F_5), -168.7 (m, *m*-F, C_6F_5). Anal. Calc for $\text{C}_{68}\text{H}_{99}\text{BF}_{20}\text{O}_{11}\text{Zr}_3 \cdot 1/2\text{CH}_3\text{CN}$: C, 46.32; H, 5.70. Found: C, 46.75; H, 5.85.

Attempts to Vary the Ratio $\text{Zr}(\text{O}i\text{Bu})_4:\text{B}(\text{C}_6\text{F}_5)_3$. Reaction between 1 equiv of $\text{Zr}(\text{O}i\text{Bu})_4$ and 2 equiv of $\text{B}(\text{C}_6\text{F}_5)_3$ in pentane and following the same procedure as the one described above for **3** led also to the formation of **3** (the filtrate containing $\text{B}(\text{O}i\text{Bu})(\text{C}_6\text{F}_5)_2$ and an excess of free $\text{B}(\text{C}_6\text{F}_5)_3$).

Reaction between 3 equiv of $\text{Zr}(\text{O}i\text{Bu})_4$ and 1 or 1.5 equiv of $\text{B}(\text{C}_6\text{F}_5)_3$ in pentane gave a white microcrystalline precipitate (see also synthesis of compound **5**). ^{19}F and ^{11}B NMR studies of the above solution in pentane- CD_2Cl_2 showed the formation of $\text{B}(\text{O}i\text{Bu})(\text{C}_6\text{F}_5)_2$. Nevertheless, the ^1H NMR of the precipitate showed signal attributed to different alkoxy groups in the range 1.30–1.90 ppm.

$\text{B}(\text{C}_6\text{F}_5)_3 \cdot (\text{THF})$ (4**).** This compound was crystallized by accident. It can be obtained in quantitative yield by the addition of 1 equiv of THF to a pentane solution of $\text{B}(\text{C}_6\text{F}_5)_3$.

^1H NMR (CD_2Cl_2): δ 4.25 (app. t, $J = 13.0$ Hz, 4H), 2.10 (app. t, $J = 13.1$ Hz, 4H) (in C_6D_6 , the signals are found at 3.23 and 0.91). ^{19}F NMR (CD_2Cl_2): δ -133.8 (*o*-F, C_6F_5), -157.1 (*p*-F, C_6F_5), -164.3 (*m*-F, C_6F_5) (in C_6D_6 , the signals are found at δ -132.9, -154.4 and -162.5). ^{11}B NMR (CD_2Cl_2): δ 3.3.

$[\text{Zr}_2(\text{O}i\text{Bu})_5(\mu\text{-O}i\text{Bu})_2(\mu\text{-N,N'-N}(\text{H})\text{C}(\text{CH}_3)=\text{C}(\text{H})\text{C}\equiv\text{N})]_2$ (5**).** This compound was obtained as a minor byproduct from a complex mixture of compounds in the following reaction. A solution of $\text{B}(\text{C}_6\text{F}_5)_3$ (208 mg, 0.406 mmol) in pentane (5 mL) was added dropwise to a solution of $\text{Zr}(\text{O}i\text{Bu})_4$ (313 mg, 0.816 mmol) in pentane (5 mL) at room temperature and was stirred for 1 day.

The solution was left 3 more days at room temperature, during which time a white precipitate was formed. The precipitate was filtered off, washed with pentane, and dried under vacuum (see above). The filtrate was dried under vacuum, giving an oil that further solidified. Spectroscopic studies (^1H , ^{19}F , and ^{11}B NMR) showed signals corresponding to unreacted $\text{Zr}(\text{O}i\text{Bu})_4$, $\text{B}(\text{O}i\text{Bu})(\text{C}_6\text{F}_5)_2$, and other unidentified species. Addition of acetonitrile to this solid caused gas evolution and formation of crystals of **5** in very low yield (5–10 mg, which precluded further analysis), suitable for X-ray diffraction studies.

$[\text{Zr}(\text{O}i\text{Bu})_3(\mu\text{-O}i\text{Bu})(\mu\text{-N}\equiv\text{CCH}_3)]_2$ (6**).** A clear solution of $\text{Zr}(\text{O}i\text{Bu})_4$ was obtained by addition of 40 mg of dichloromethane to $\text{Zr}(\text{O}i\text{Bu})_4$ (150 mg, 0.3909 mmol), followed by addition of 2 mL of acetonitrile. This solution became more viscous and cloudy within hours, and crystals of **6** suitable for X-ray diffraction analysis were obtained. Complex **6** could not be isolated because it loses the coordinated acetonitrile molecules upon vacuum, re-forming $\text{Zr}(\text{O}i\text{Bu})_4$.

$[\text{Zr}(\text{O}i\text{Bu})_2\{\mu\text{-O}(\text{O}i\text{Bu})\text{B}(\text{C}_6\text{F}_5)_2\}]_2$ (7**).** Solid $\text{HOB}(\text{C}_6\text{F}_5)_2$ (56 mg, 0.15 mmol) was added to a solution of $\text{Zr}(\text{O}i\text{Bu})_4$ (59 mg, 0.15 mmol) in CH_2Cl_2 (2 mL) at room temperature. The reaction mixture was stirred for 24 h at room temperature. Slow evaporation afforded white crystals of **7**. The crystals were filtered off, washed with THF, and dried under vacuum. Yield: 55 mg (55%). ^1H NMR (CD_2Cl_2): δ 1.41 (s, 9H, $\text{BO}i\text{-Bu}$); 1.27 (s, 18H, *Ot*-Bu). ^{19}F NMR (CD_2Cl_2): δ -54.8 (br, *o*-F, C_6F_5), -82.3 (*p*-F, C_6F_5), -88.6 (*m*-F, C_6F_5). ^{11}B NMR (CD_2Cl_2): δ 5.0. Anal. Calc for $\text{C}_{24}\text{H}_{27}\text{BF}_{10}\text{O}_4\text{Zr}$: C, 42.93; H, 4.05. Found: C, 42.74; H, 3.83.

Acknowledgment. We are grateful to the CNRS for financial support.

Supporting Information Available: CIF files and tables of atomic coordinates, bond distances, and angles for the X-ray crystal structures of complexes **1–7**. This material is available free of charge via the Internet at <http://pubs.acs.org>.

OM800234Z